Article

Rational Design of A Stimuli-Responsive Polymer Electrode Interface Coupled With In Vivo Microdialysis for Measurement of Sialic Acid in Live Mouse Brain in Alzheimer's Disease

Shushu Ding, Sumei Cao, Yingzi Liu, Ying Lian, Anwei Zhu, and Guoyue Shi

ACS Sens., **Just Accepted Manuscript** • DOI: 10.1021/acssensors.6b00772 • Publication Date (Web): 22 Feb 2017

Rational Design of A Stimuli-Responsive Polymer Electrode Interface Coupled With In Vivo Microdialysis for Measurement of Sialic Acid in Live Mouse Brain in Alzheimer's Disease

Shushu Ding,† Sumei Cao,† Yingzi Liu,‡ Ying Lian,† Anwei Zhu*† and Guoyue Shi*†

†School of Chemistry and Molecular Engineering, East China Normal University, 500 Dongchuan Road, Shanghai 200241, People's Republic of China.

‡Institute of Brain Functional Genomics, East China Normal University, 3663 Zhongshan Road N., Shanghai 200062, People's Republic of China.

KEYWORDS. sialic acid, stimuli-responsive polymer, electrochemical sensor, microdialysis, Alzheimer's disease

ABSTRACT: Sensitive and selective monitoring of sialic acid (SA) in cerebral nervous system is of great importance for studying the role that SA plays in the pathological process of Alzheimer's disease (AD). In this work, we first reported an electrochemical biosensor based on a novel stimuli-responsive copolymer for selective and sensitive detection of SA in mouse brain. Notably, through synergetic hydrogen-bonding interactions, the copolymer could translate the recognition of SA into their conformational transition and wettability switch, which facilitated the access and enrichment of redox labels and targets to the electrode surface, thus significantly improving the detection sensitivity with the detection limit down to 0.4 pM. Besides amplified sensing signals, the proposed method exhibited good selectivity toward SA in comparison to potential interference molecules coexisting in the complex brain system due to the combination of high affinity between phenylboronic acid (PBA) and SA and the directional hydrogen-bonding interactions in the copolymer. The electrochemical biosensor with remarkable analytical performance was successfully applied to evaluate the dynamic change of SA level in live mouse brain with AD combined with in vivo midrodialysis. The accurate concentration of SA in different brain regions of live mouse with AD has been reported for the first time, which is beneficial for progressing our understanding of the role that SA plays in physiological and pathological events in the brain.

As one of the most fatal diseases, Alzheimer's disease (AD) has been considered as a serious social and healthy problem.[1] Although the pathology of AD is not clearly understood, sialic acid (SA) has been proposed to be closely related to AD. On one hand, sialic acid residues on the terminal position of brain gangliosides work as bridges for the binding between ganglioside and amyloid-β (Aβ), which promote a conformational transition of Aβ, and then catalyze the formation of neurotoxic fibrils.[2,3] Importantly, it has been reported that the number of binding sites is roughly proportional to the number of SA residues.[4] On the other hand, AD is characterized by the selective neuronal death and brain shrinkage. These pathological changes are accompanied by the reduction in the level of SA due to the enrichment of gangliosides in neurons.[5,6] In this regard, the development of an effective method for detecting cerebral SA is necessary to enhance our understanding of the role that SA plays in brain activity and to diagnose human brain injuries of AD.

The current protocols for cerebral SA detection mostly rely on colorimetric resorcinol method with brain tissue.[7] However, it is a post-mortem examination that needs toxic reagents and complicated sample pretreatment. Although several attempts have also been made to detect SA on live cells, the low specificity of lectins,[8] time-consuming procedure,[9,10] and the indirect and complicated sensing through in situ chemical modification of SA on cells[11,12] restrain the suitability of them for monitoring of SA in vivo. Microdialysis, a minimally-invasive sampling technique that is used for continuous measurement of small-molecular-weight substances concentrations in interstitial tissue fluid, is one of the few techniques that permits quantification of biomolecules in living animals.[13] Profiting from facile operation and direct sampling, microdialysis has been combined with electrochemical sensor to realize near real-time monitoring of the dynamic changes in the level of several biomolecules in brain microdialysates.[14] However, to the best of our knowledge, there has been no report about the exploration of electrochemical assays combined with microdialysis for SA detection in live mouse brain with AD, probably because the complexity of cerebral system necessitates the proposed methods with significant analytical performance, particularly in sensitivity and selectivity.

Phenylboronic acid (PBA) has been demonstrated to selectively react with SA at physiological pH with high stability.[15-20] This anomalous selectivity is correlated to the

formation of intermolecular B-N or B-O bonds between the boron atom and the amide group of SA at the C-5 position, which is significantly different from other monosaccharide.[21] Recently, one kind of PBA homopolymer (comprising single type of polymer chain) has been employed for potentiometric detection of SA in serum.[22] But unfortunately, this polymer assembled by electropolymerization showed poor controllability owing to its vulnerability to different deposition conditions, and even worse, long time to stabilize electrochemical potential before analysis[23] and relatively low sensitivity to the analyte was encountered. Therefore, this PBA homopolymer was disadvantageous for SA detection in complicated environment. Compared with PBA homopolymer, stimuli-responsive copolymers, designed by the "recognition-mediating-function" (RMF) concept, have emerged recently as a fascinating sensing platform in recognition and analysis because of their ease of preparation, improvement of sensing performance, and simple surface modification in fabrication of devices.[24-27] However, no studies about the exploration of stimuli-responsive polymers to electrochemical monitoring of SA were reported. Inspired by our early study,[28] we designed a new three-component copolymer which contained PBA as the specific recognition unit, the bis(trifluoromethyl)-modified phenylthiourea (TP) as the mediating unit, and poly(*N*-isopropylacrylamide) (PNI) as the functional switching unit for the detection of SA. In contrast to electropolymerization method, this copolymer was immobilized onto the electrode surface via Au-S covalent bond, displaying better controllability and stability. Besides, apart from the specific covalent bonding between PBA and SA, TP unit, a strong hydrogen-bonding effector, contributed to the formation of directional hydrogen bonds, improving the selectivity toward SA recognition. Moreover, the copolymer could translate the specific recognition of SA into its conformational transition and wettability switch by synergetic hydrogen-bonding interactions, which facilitated the access and enrichment of redox labels and targets to the electrode surface, leading to a highly sensitive electrochemical assay (Figure 1).

Herein, we assembled a novel three-component copolymer onto gold flower-like film-modified screen-printed carbon electrode (SPCE) to develop a sensitive and selective electrochemical assay and further successfully applied it to evaluate the SA level in live mice brain with AD by combining with in vivo microdialysis (Figure 1). Notably, this kind of stimuli-responsive copolymer modified on the electrode surface not only demonstrated remarkable recognition ability but also worked as a signal amplification strategy. Additionally, the gold flower-like film electrodeposited on the SPCE surface dramatically enhanced the surface roughness of the substrate,[29,30] which amplified the inherent wettability of the surface-attached copolymer and thus improved the sensitivity toward SA to fulfil the requirement for in vivo detection. Furthermore, known as an effective and nondestructive tool to probe the electron-transfer and electrical properties of thin films,

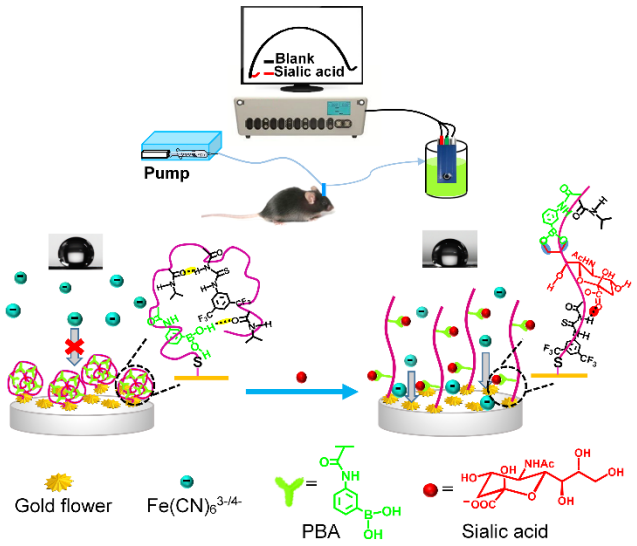

Figure 1. Schematic illustration of the electrochemical biosensor coupled with in vivo microdialysis for measurement of SA in live mouse brain. The recognition of sialic acid changed the conformation and wettability of the copolymer by synergetic hydrogen-bonding interactions, leading to the access and enrichment of redox labels, and to a sensitive EIS detection based on a decrease in the electron transfer resistance.

electrochemical impedance spectroscopy (EIS) was employed to quantify SA based on the change of the charge transfer resistance (R_{ct}) with high sensitivity.[31-36] More interestingly, the R_{ct} value decreased after the addition of SA, effectively avoiding the inaccuracy signal by potential interferences, which often bring non-specific adsorption and large R_{ct}.[37] Accordingly, the excellent analytical performance of this electrochemical biosensor, together with the unique properties of microdialysis, established a sensitive and selective method for evaluating SA levels in different brain regions of live mice with AD. As far as we know, this is the first report of an electrochemical biosensor that determines the SA level associated with AD based on a stimuli-responsive copolymer. The concentration of SA in prefrontal cortex and hippocampus of AD mice decreased by about 2.8-fold and 1.7-fold, respectively, compared with those in the normal mouse brains.

EXPERIMENTAL SECTION

Reagents and Materials. Sialic acid (SA), neuraminidase (NEU), ascorbate acid (AA), dopamine (DA), 5-hydroxytryptamine (5-HT), lactate, 3,4-dihydroxyphenylacetic acid (DOPAC), glucose, galactose, mannose, amino acids, transferrin (TF), *N*-isopropyl acrylamide (NIPAM) and *S*-benzyl dithiobenzoate (BDTB) were purchased from Sigma-Aldrich. A Lyphochek hemoglobin A1C (HbA1c) linearity set was bought from Bio-Rad Laboratories. *N*-acetyl-2-*O*-methyl-*β*-D-*N*-acetylneuraminic acid was purchased from Alfa Chemistry. Chloroauric acid ($HAuCl_4 \cdot 4H_2O$), 2,2'-azobisisobutyronitrile (AIBN), potassium hexacyanoferrate (II) ($K_4[Fe(CN)_6] \cdot 3H_2O$), potassium

hexacyanoferrate (III) ($K_3[Fe(CN)_6]$) were obtained from Sinopharm Chemical Reagent Co., Ltd. Peroxidase from horseradish (HRP), sodium borohydride ($NaBH_4$) and all metallic salts were obtained from Aladdin. NIPAM was recrystallized in hexane for three times before use. Acryloyl-3,5-bis(trifluoromethyl)phenylthiourea (Ac-TP) and acryloyl-3-amidophenylboronic acid (Ac-PBA) were respectively synthesized based on the method previously reported.[38,39] Artificial cerebrospinal fluid (aCSF) was prepared by mixing NaCl (126 mM), KCl (2.4 mM), KH_2PO_4 (0.5 mM), $MgCl_2$ (0.85 mM), $CaCl_2$ (1.1 mM), $NaHCO_3$ (27.5 mM), and Na_2SO_4 (0.5 mM) into doubly distilled water, and then we adjusted the solution pH to 7.4. Other reagents were of analytical grade. All aqueous solutions were prepared from doubly distilled water (18 MΩ cm, Hitech science tool laboratory water purification system).

Instruments and Methods. X-ray photoelectric spectroscopy (XPS) was taken on a Kratos Axis Ultra DLD spectrometer with Al Kα source (1486.6 eV). Atomic force microscope (AFM) images were obtained on a flat gold substrate modified with copolymer by using a Bruker Multimode 8 AFM in the tapping mode. Surface morphological images were taken using a HITACHI S-4800 scanning electron microscope (SEM). ^{1}H NMR spectra were collected in d6-DMSO on a Bruker AV-500 instrument. Fourier transform (FTIR) spectra was performed on a NEXUS 670 spectrometer. X-ray diffraction (XRD) was carried out on a Bruker D8 ADVANCE instrument. Static contact angle was measured on a JC2000A contact angle meter (Shanghai Zhongchen Digital Technology Co. Ltd., China). The molecular weight was obtained from a gel permeation chromatography (GPC) equipped with a Waters 1515 isocratic HPLC pump, a Waters 2414 refractive index detector (RI), and a set of Waters Styragel columns. Tetrahydrofuran (THF) was used as the solvent for the copolymer and the eluent for GPC with a flow rate of 1.0 mL/min at 30 °C. All electrochemical measurements were performed on a Metrohm Autolab PGSTAT302N potentiostat-galvanostat with a software NOVA 1.9 at 25 °C. The screen-printed carbon electrode (SPCE, Zensor R&D Co., Ltd., Taiwan) used for modification was consisted of a graphite working electrode (diameter: 3 mm), an Ag|AgCl reference electrode and a graphite auxiliary electrode. The insulating layer around the working area constituted an electrochemical microcell. Electrochemical impedance spectroscopy (EIS) experiments were performed in 0.1 M aCSF buffer solution containing equimolar (5 mM) $[Fe(CN)_6]^{3-/4-}$, and experimental conditions were as follows: open-circuit potential, 0.14 V; alternative voltage, 5 mV; frequency range, 0.01–10^5 Hz.

Preparation of PNI-PBA-TP Copolymer. Copolymer was synthesized by reversible addition-fragmentation chain transfer (RAFT) polymerization. In a typical run, NIPAM, Ac-PBA, Ac-TP, BDTB and AIBN were added into a mixture of 1,4-dioxane/methanol (4:1) in the molar ratio of 170:15:15: 2: 1. After being degassed three times, the mixture was kept at 70 °C for 20 h. Then, chloroform was added to halt the polymerization. The obtained copolymer (denoted as PNI-PBA-TP) was precipitated by adding excess amount of hexane. The precipitate was redissolved in a small amount of chloroform and then reprecipitated by hexane. This precipitation procedure was repeated three times. The powdery products with light pink color were dried under vacuum overnight.

Preparation and Modification. First of all, gold flower-like nanostructures were electrochemically deposited on SPCEs at –0.08 V for 3 min in 40 mM $HAuCl_4$ solution. The electrode electrodeposited with Au was symbolized as SPCE/Au. Subsequently, copolymer was immobilized onto the above electrode surface via Au-S bond to obtain SPCE/Au/PNI-PBA-TP. Briefly, thiolated copolymer was prepared by adding 20 mg of PNI-PBA-TP into 10 mL of methanol containing 2 mM $NaBH_4$ followed by being incubated for 2 h at 4 °C. Then, SPCE/Au was immersed in the copolymer solution for 60 min. For removing the excess copolymer over the surface, the modified electrode was washed with methanol, distilled water and dried under a flow of nitrogen and denoted as SPCE/Au/PNI-PBA-TP.

In Vivo Microdialysis. All experiments involving animals were performed following the approval of the Animal Ethics Committee in ECNU, China. Female C57BL/6J mice at 12 months of age and female APP/PS1 double transgenic mice with the same age were purchased from Shanghai Research Center for Model OrganisBILITm and were housed under standard environmental conditions (12 h light/dark cycle, 22°C) with food and water ad libitum. Surgeries for in vivo microdialysis were performed as reported previously.[40] Briefly, the animals were anaesthetized with sodium pentobarbital (50 mg kg^{-1}, i.p.) and wrapped in a homeothermic blanket (Beijing Tide-Gene Biotechnology Development Center). Then, the animal was positioned onto a stereotaxic frame. Bore hole (0.75 mm) was made above the right prefrontal cortex (bregma 2.8 mm, 1.5 mm lateral to midline, and 1.5 mm below dura) and left hippocampus (bregma –2.3 mm, 2.5 mm lateral to midline, and 1.8 mm below dura) according to a mouse brain atlas.[41] Next, 30 μL of aCSF containing NEU (4 U/mL) was applied by three equal injections of 10 μL volume at 5 min intervals into the prefrontal cortex and hippocampus and the mouse kept anesthesia for 2 h. Finally, the CMA 7 microdialysis probes were implanted. The aCSF solution was infused at the flow rate of 2.0 μL/min. After equilibration for 90 min, the microdialysates were collected at 30 min intervals for cerebral SA determination. All the measurements were reproduced for five times, presented as mean ±S.D. (n=5)

RESULTS AND DISCUSSION

Synthesis and Characterization of PNI-PBA-TP. Based on the "recognition-mediating-function" (RMF) design concept reported in our early study,[28] a novel stimuli-responsive copolymer containing phenylboronic acid (PBA) as the recognition unit, the bis(trifluoromethyl)-modified phenylthiourea (TP) as the mediating unit, and poly(*N*-isopropylacrylamide) (PNI) as the functional switching unit

was synthesized via reversible addition-fragmentation chain-transfer (RAFT) polymerization as described in the Experimental Section, which was denoted as PNI-PBA-TP. The structure of PNI-PBA-TP was characterized by fourier transform infrared spectrometer (FT-IR) and nuclear manetic resonance (NMR). In the FT-IR spectra (Figure S2), besides the signals of 1360 and 1455 cm^{-1} m which were assigned to B-O stretching vibration, the peaks corresponding to the bending vibration of B-O were observed at 986 and 1047 cm^{-1}. Moreover, the typical absorption of O-H in PBA unit was clearly found at 3305 cm^{-1}. In addition, the peaks attributed to C-F and C=S vibration in TP unit located at 1279 and 1135 cm^{-1}, while the stretching vibration of $-CH_3$ in PNI unit appeared at 2935 and 2974 cm^{-1}. All these results reflected the existence of three units in the copolymer chains. Besides, ^1H NMR also confirmed the successful polymerization between three monomers (Figure S3). The number-average molecular weight M_n was estimated by gel permeation chromatography (GPC) as 8536 (M_w/M_n=1.10).

Characterization of the Modified SPCE. The modification of electrode was described in the Experimental Section. Initially, a gold flower-like film was electrodeposited on the screen-printed carbon electrode (SPCE) surface, which was referred to as SPCE/Au. As shown in the SEM images (Figure S4A), the gold flowers with a diameter of about 900 nm were uniformly distributed on the SPCE surface, which significantly increased the roughness of the substrate. The X-ray diffraction (XRD) pattern displayed three sharp peaks corresponding to (111), (200), and (220) (Figure S4B), which revealed the pure crystalline characteristic of gold flowers. Then, the copolymer was immobilized onto the above electrode surface via Au-S bond to obtain SPCE/Au/PNI-PBA-TP. As shown in Figure S5, two obvious peaks in X-ray photoelectric spectroscopy (XPS) were obtained at 191.5 eV for B1s and at 688.2 eV for F 1s respectively, which were assigned to B-O and C-F bonds of PBA and TP units in the copolymer. In addition, compared with the gold flower-like film with a water contact angle of 68° (Figure 2A), the copolymer-modified electrode showed hydrophobicity with a water contact angle of 126.1°, because of the hydrophobic property of the exposing alkane chains[42] and the large roughness factor of the gold flower-like film (Figure 2A). These results confirmed that PNI-PBA-TP copolymer was successfully modified on the electrode.

Enhanced Electrochemical Detection of Sialic Acid. As a stimuli-responsive polymer, PNI-PBA-TP could undergo morphology and wettability changes upon recognition of SA via tunable hydrogen-bonding interactions. As illustrated by atomic force microscopy (AFM) images, initially, the copolymer on the Au surface exhibited a particle-like morphology with film thickness about 10 nm due to the formation of intramolecular hydrogen bonds among three units (Figure 2C). Whereas, after being treated by SA solution, PBA would selectively interact with SA through covalent bonds, which were enhanced by

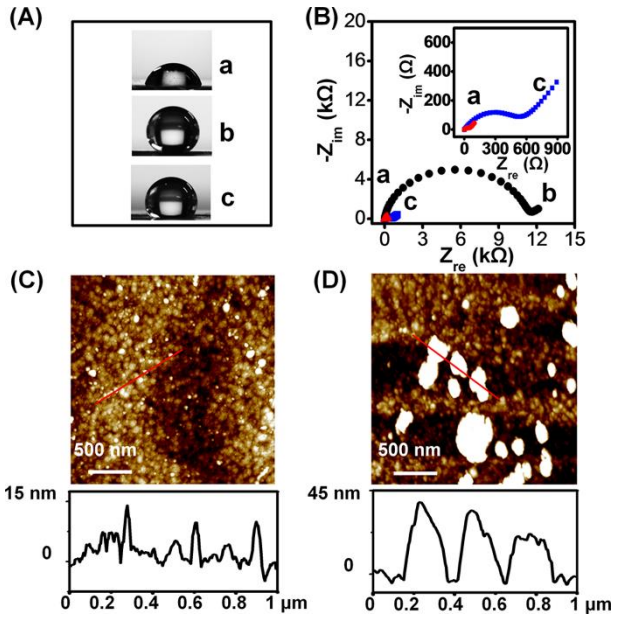

Figure 2. (A) Contact angle photographs and (B) Nyquist plots obtained at (a) SPCE/Au surface, SPCE/Au/PNI-PBA-TP surface (b) before and (c) after being exposed to SA solution (1×10^{-5} M) and typical tapping-mode AFM images for the copolymer modified Au surface (C) before and (D) after being treated by SA solution (1×10^{-3} M) together with the height profiles of the cross-section analysis.

hydrogen-bonding interactions between TP and SA, resulting in the breakdown of intramolecular hydrogen bonds within PNI units. Hence, the film swelled with its thickness increasing to about 35 nm (Figure 2D). Meanwhile, the water contact angle of SPCE/Au/PNI-PBA-TP surface decreased to about 115° (Figure 2A). This result clearly demonstrated that the copolymer film exhibited wettability response to SA. To demonstrate the rationality and necessity of gold-flower like film, a blank experiment on smooth gold film modified with the copolymer was performed. It was found that the gold flower-like film surface exhibited a more substantial wettability switching than a smooth gold film surface in SA detection (Figure S6), thus pointing out the importance of gold flower with large roughness factor for enhancing the SA responsiveness. However, considering the limitation of static contact angle measurements in sensitivity, an elegant method sensitive to conformational changes of polymer chains and their wettability switch on interfaces is essentially demanded for the signal amplification of SA recognition.

Electrochemical impedance spectroscopy (EIS) is a powerful tool to probe the electron transfer and electrical properties of thin films. To sensitively detect and quantify SA, EIS was further employed based on the change of charge-transfer resistant (R_{ct}). The results were demonstrated as Nyquist plots. The diameter of semi-circular part of the plot corresponds to the R_{ct} at electrode surface and could be calculated by fitting Randles circuit (Figure S7). As expected, PNI-PBA-TP copolymer on the SPCE surface retarded the electron transfer of redox probe and remarkably

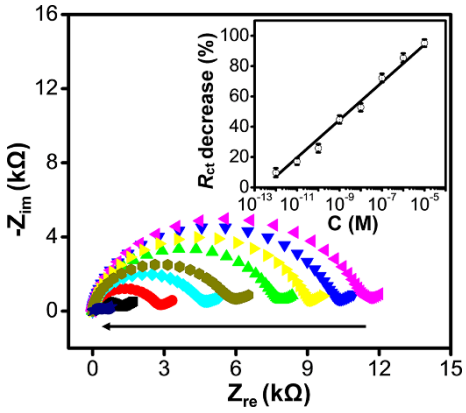

Figure 3. Nyquist plots obtained at the modified electrode surfaces in artificial cerebrospinal fluid (aCSF, pH 7.4) containing 5 mM $Fe(CN)_6^{3-/4-}$ upon addition of SA solutions (1×10^{-12}–1×10^{-5} M). Inset: relationship between the extent of R_{ct} decrease and the concentrations of SA. Error bars represent standard error measurements (s.e.m.).

increased the R_{ct} to be 11.1 kΩ. After being exposed to SA solutions, the R_{ct} dropped down to 576 Ω (Figure 2B). This may result from the conformation and wettability changes on the copolymer modified electrode surface, which enhanced the permeability and diffusion of electroactive probe through the polymer and thus facilitated its interface redox reaction. This observation is just the proof-of-concept for assaying of SA by the EIS method. Cyclic voltammetry (CV) of SPCE/Au/PNI-PBA-TP in the absence and presence of SA also proved the working principle, as demonstrated in Figure S8. In addition, experiments for monitoring of SA were also optimized by varying the polymerization time of PNI-PBA-TP,[43] the modification time of copolymers onto SPCE surface, and the reaction time of SA (Figure S10-12).

Moreover, the PNI-PBA-TP on the electrode surface not only acted as a recognition element for SA but also amplified the SA-induced electrochemical signal. Compared with conventional methods, which were solely based on the binding for SA with receptor, the SA-induced wettability further promoted the enrichment and binding of SA on electrode surface, thus substantially improving the detection sensitivity. Besides, the gold flower-like film also contributed to the enhanced electrochemical response for SA detection (Figure S6 and Figure S13). As shown in Figure 3, R_{ct} values gradually decreased as the SA concentration increased. The detection linear range for SA extended from 1×10^{-5} M to 1×10^{-12} M, and the detection limit could be achieved as low as 0.4 pM, which was lower than those obtained by other methods (Table S1) and met the requirement for sensitive monitoring of cerebral SA in mouse brain. Reproducibility has been tested with six different SPCE/Au/PNI-PBA-TP electrodes for 10^{-5} M SA. The relative standard deviation (RSD) was 1.43%, indicating the SPCE/Au/PNI-PBA-TP electrodes had good reproducibility. Cycling experiments for alternately treating the electrode surface by SA and pure water demonstrated that the

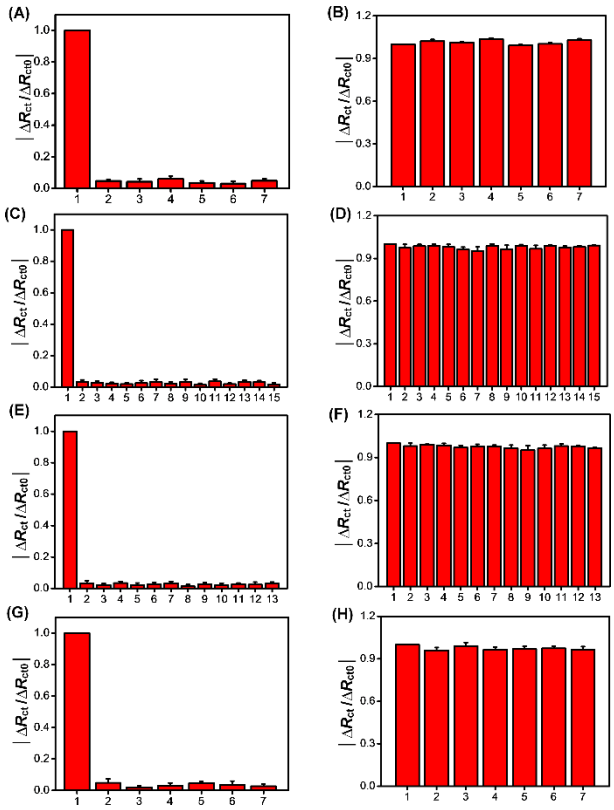

Figure 4. Selectivity and competition experiments for SPCE/Au/PNI-PBA-TP toward (A) and (B) monosaccharides (1-7: SA, glucose, mannose, galactose, fucose, xylose, fructose, 1 mM for other monosaccharides, 10 μM for SA), (C) and (D) metal ions (1-15: SA, K^+, Ca^{2+}, Na^+, Mg^{2+}, Zn^{2+}, Cu^{2+}, Co^{2+}, Fe^{3+}, Fe^{2+}, Mn^{2+}, Ni^{2+}, Cd^{2+}, Al^{3+}, Ag^+, 1 mM for K^+, Ca^{2+}, Na^+, Mg^{2+}; 10 μM for other metal ions; 10 μM for SA), (E) and (F) amino acids (1-13: SA, Glu, Gly, Phe, Met, Val, Cys, His, Iso, Arg, Lys, Leu, Tyr, 10 μM for all species), or (G) and (H) other biological molecules (1-7: 10 μM SA, 50 μM AA, 20 μM UA, 20 μM DA, 50 μM DOPAC, 20 μM 5-HT, 1 mM lactate). The left bars (A), (C), (E), (G) represent the ratio between the charge-transfer resistance change of the SPCE/Au/PNI-PBA-TP induced by potential interferences and the charge-transfer resistance change of the SPCE/Au/PNI-PBA-TP induced by sialic acid. The right bars (B), (D), (F), (H) refer to the charge-transfer resistance change of the SPCE/Au/PNI-PBA-TP upon addition of both potential interferences and sialic acid divided by the charge-transfer resistance change of the SPCE/Au/PNI-PBA-TP induced by sialic acid alone. ΔR_{cto} represents the charge-transfer resistance change induced by sialic acid, ΔR_{ct} represents the charge-transfer resistance change induced by potential interferences (A), (C), (E), (G) or the mixture of potential interference and sialic acid (B),(D),(F),(H).

R_{ct} could revert back to the original value after further treatment, so the electrode can be reused (Figure S15).

As is known that the brain system is very complex, it presents a significant challenge to the established method not only in sensitivity, but more importantly in selectivity. In this work, the selectivity for SA was displayed by the charge-transfer resistance change (ΔR_{ct}) induced by

potential interferences over the charge-transfer resistance change (ΔR_{cto}) by SA. First, various monosaccharides which are necessary for the brain functioning were examined. As shown in Figure 4, these monosaccharides showed negligible responses. In addition, no obvious responses were observed for metal ions, amino acids and biological species that commonly coexist in biological system. For the competition test, all these potential interferences produced no discernible changes in the electrochemical response for SA, indicating the high selectivity of the present method. The reasons for the anomalous selectivity may be as follows: first, the binding constant of 37.6 between PBA and SA was 2–7 times higher than those for other sugars at physiological pH of 7.4.[21,22] Second, TP unit in the copolymer may not only interacted with hydroxyl groups of SA through directional hydrogen bonds but also combined with the carboxylate ion (-COO$^-$) of SA,[38,44] thus improving the selectivity toward SA recognition.

Monitoring Cerebral Sialic Acid in Rat Brain Microdialysates. It has been reported that SA participated in many neuronal processes including axonal growth, neurotransmitters synthesis and synaptic transmission.[45,46] The advantages of high sensitivity and selectivity of the developed electrochemical sensor incited us to further access its performance in monitoring SA level in central nervous system. For in vivo measurement of SA in mouse brain, neuraminidase (NEU) was employed to cleave terminal SA residues of glycoconjugates into extracellular fluid and the free SA was sampled and quantified by in vivo microdialysis.[47,48] As shown in Figure 5A, for normal mice, the R_{ct} values progressively decreased and reached its minimum at 240 min. This dynamic change could be attributed to the increasing level of SA cleaved from cell surface upon NEU treatment.[47] Based on the calibration curve and the microdialysis recovery (17 %) measured in the same experiment, the maximum concentration of SA in dialysates from the prefrontal cortex of normal mice were observed to be 17 ± 0.88 μM. Although the dynamic changes of SA level in the mouse brains with AD displayed the same trend, the maximum concentration of SA in dialysates was evaluated to be 6.17 ± 0.52 μM, which decreased by about 2.8-fold compared with that in the normal mouse brains. Meanwhile, the microdialysates from the hippocampus were also measured (Figure S17). Like in prefrontal cortex, the SA concentration in dialysates from the hippocampus for AD mice decreased by about 1.7-fold compared with normal animals. Considering the role SA played in promoting learning ability and memory formation,[49] the cognitive decline associated with AD might be related with the decreasing level of SA although the mechanism is still unknown. These results further validate our electrochemical biosensor as an effective platform for in vivo evaluating SA level and exploring the changes that occur in neurodegenerative diseases.

CONCLUSIONS

In summary, a sensitive and selective electrochemical assay for SA has been developed based on the specific

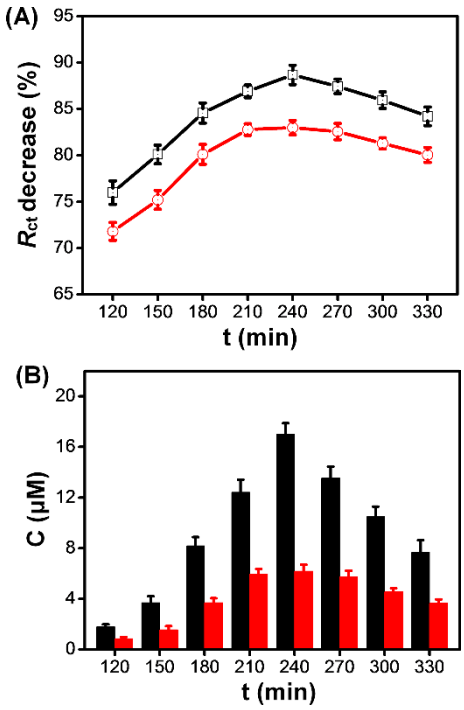

Figure 5. (A) Time-dependent R_{ct} decrease extent at the modified electrode surfaces for determination of SA in the prefrontal cortex of normal mouse brains (black curve) and mouse brains with AD (red curve). (B) Time-dependent changes in the SA level in the prefrontal cortex of normal mouse brains (black column) and mouse brains with AD (red column). Error bars represent standard error measurements with n = 5.

recognition of PBA to SA and the amplified property of the stimuli-responsive copolymer. By combining with in vivo microdialysis, this electrochemical biosensor with remarkable analytical performance was proved to be an efficient approach for measurement of SA in living mouse brain. This study has first measured the concentration of SA in prefrontal cortex and hippocampus of live mice with or without AD, which may have a close relationship with physiological and pathological events in the brain. The potential of this electrochemical method in dynamic monitoring the changes in the level of SA in live mouse brain should enable it to study broad brain functions of SA under different physiological conditions. The present work has also provided the rational design and construction of electrodes for quantitative in vivo monitoring of other molecules related to brain disease since the "recognition-mediating-function" (RMF) design principle for the copolymer makes it easy to change the copolymer structure.

ASSOCIATED CONTENT

Supporting Information. Characterization of PNI-PBA-TP copolymer, characterization of the electrode modification process, amplified wettability of gold flower-like film, equivalent circuit, cyclic voltammetry for proving the working principle, the role of TP unit in the copolymer, optimized conditions, enhanced electrochemical response on the gold flower-

like nanostructure, stability test, cycling experiment, selectivity test towards glycoproteins, determination of SA level in the hippocampus of living mouse brains, comparison of the performance of different methods for the determination of SA. The Supporting Information is available free of charge on the ACS Publications website. This material is available free of charge via the Internet at http://pubs.acs.org.

AUTHOR INFORMATION

Corresponding Author

* E-mail: awzhu@chem.ecnu.edu.cn. Tel: +86-21-54340042. Fax: +86-21-54340042
* E-mail: gyshi@chem.ecnu.edu.cn.

Notes

The authors declare no competing financial interest.

ACKNOWLEDGMENT

This work was supported by the National Natural Science Foundation of China (21405048, 21675053, 21635003), "Yang Fan" Project funded by Science and Technology Commission of Shanghai Municipality (14YF1404000), and China Postdoctoral Science Foundation (2016T90349, 2014M550225).

REFERENCES

(1) Yu, Y.; Zhang, L.; Li, C.; Sun, X.; Tang, D.; Shi, G. A Method for Evaluating the Level of Soluble β-Amyloid$_{(1-40/1-42)}$ in Alzheimer's Disease Based on the Binding of Gelsolin to b-Amyloid Peptides. *Angew. Chem., Int. Ed.* **2014**, *53*, 1-5.

(2) Matsuzaki, K.; Horikiri, C. Interactions of amyloid β-peptide $_{(1-40)}$ with ganglioside-containing membranes. *Biochemistry* **1999**, *38*, 4137-4142.

(3) Choo-Smith, L. P.; Garzon-Rodriguez, W.; Glabe, C. G.; Surewicz, W. K. Acceleration of amyloid fibril formation by specific binding of Abeta-(1-40) peptide to ganglioside-containing membrane vesicles. *J. Biol. Chem.* **1997**, *272*, 22987-22990.

(4) Kakio, A.; Nishimoto, S.; Yanagisawa, K.; Kozutsumi, Y.; Matsuzaki, K. Interactions of amyloid β-protein with various gangliosides in raft-like membranes: importance of GM1 ganglioside-bound form as an endogenous seed for Alzheimer amyloid. *Biochemistry* **2002**, *41*, 7385-7390.

(5) Ariga, T.; McDonald, M. P.; Yu, R. K. Thematic Review Series: Sphingolipids. Role of ganglioside metabolism in the pathogenesis of Alzheimer's disease—a review. *J. Lipid Res.* **2008**, *49*, 1157-1175.

(6) Lacomba, R.; Salcedo, J.; Alegría, A.; Lagarda, M. J.; Barberá, R.; Matencio, E. Determination of sialic acid and gangliosides in biological samples and dairy products: a review. *J. Pharmaceut. Biomed.* **2010**, *51*, 346-357.

(7) Svennerholm, L. Quantitive estimation of sialic acids: II. A colorimetric resorcinol-hydrochloric acid method. *Biochim. Biophys. Acta.* **1957**, *24*, 604-611.

(8) Kohler, J. J. Aniline: a catalyst for sialic acid detection. *Chem. Bio. Chem.* **2009**, *10*, 2147-2150.

(9) Shen, P.; Hsu, J.; Chen, S. Dimethyl isotope-coded affinity selection for the analysis of free and blocked N-termini of proteins using LC-MS/MS. *Anal. Chem.* **2007**, *79*, 9520-9530.

(10) Xiong, Z.; Qin, H.; Wan, H.; Huang, G.; Zhang, Z.; Dong, J.; Zhang, L.; Zhang, W.; Zou, H. Layer-by-layer assembly of multilayer polysaccharide coated magnetic nanoparticles for the selective enrichment of glycopeptides. *Chem. Commun.* **2013**, *49*, 9284-9286.

(11) Zeng, Y.; Ramya, T. N. C.; Dirksen, A.; Dawson, P. E.; Paulson, J. C. High-efficiency labeling of sialylated glycoproteins on living cells. *Nat. Methods.* **2009**, *6*, 207-209.

(12) Hangauer, M. J.; Bertozzi, C. R. A FRET-Based Fluorogenic Phosphine for Live-Cell Imaging with the Staudinger Ligation. *Angew. Chem., Int. Ed.* **2008**, *47*, 2394–2397.

(13) Yang, C.; Chang, C.; Tsai, P.; Chen, W.; Tseng, F.; Lo, L. Nanoparticle-based in vivo investigation on blood-brain barrier permeability following ischemia and reperfusion. *Anal. Chem.* **2004**, *76*, 4465–4471.

(14) Lin, Y.; Zhu, N.; Yu, P.; Su, L.; Mao, L. Physiologically relevant online electrochemical method for continuous and simultaneous monitoring of striatum glucose and lactate following global cerebral ischemia/reperfusion. *Anal. Chem.* **2009**, *81*, 2067-2074.

(15) Matsumoto, A.; Sato, N.; Kataoka, K.; Miyahara, Y. Noninvasive sialic acid detection at cell membrane by using phenylboronic acid modified self-assembled monolayer gold electrode. *J. Am. Chem. Soc.* **2009**, *131*, 12022-12023.

(16) Deshayes, S.; Cabral, H.; Ishii, T.; Miura, Y.; Kobayashi, S.; Yamashita, T.; Matsumoto, A.; Miyahara, Y.; Nishiyama, N.; Kataoka, K. Phenylboronic acid-installed polymeric micelles for targeting sialylated epitopes in solid tumors. *J. Am. Chem. Soc.* **2013**, *135*, 15501-15507.

(17) Wu, X.; Li, Z.; Chen, X.; Fossey, J. S.; James, T. D.; Jiang, Y. Selective sensing of saccharides using simple boronic acids and their aggregates. *Chem. Soc. Rev.* **2013**, *42*, 8032-8048.

(18) Han, E.; Ding, L.; Ju, H. Highly sensitive fluorescent analysis of dynamic glycan expression on living cells using glyconanoparticles and functionalized quantum dots. *Anal. Chem.* **2011**, *83*, 7006-7012.

(19) Cao, J.; Zhang, P.; Liu, Y.; Abdel-Halim, E. S.; Zhu, J. Versatile Microfluidic Platform for the Assessment of Sialic Acid Expression on Cancer Cells Using Quantum Dots with Phenylboronic Acid Tags. *ACS Appl. Mater. Interfaces* **2015**, *7*, 14878-14884.

(20) Chaudhary, P. M.; Murthy, R. V.; Yadav, R.; Kikkeri, R. A rationally designed peptidomimetic biosensor for sialic acid on cell surfaces. *Chem. Commun.* **2015**, *51*, 8112-8115.

(21) Otsuka, H.; Uchimura, E.; Koshino, H.; Okano, T.; Kataoka, K. Anomalous binding profile of phenylboronic acid with N-acetylneuraminic acid (Neu5Ac) in aqueous solution with varying pH. *J. Am. Chem. Soc.* **2003**, *125*, 3493-3502.

(22) Zhou, Y.; Dong, H.; Liu, L.; Liu, J.; Xu, M. A novel potentiometric sensor based on a poly (anilineboronic acid)/graphene modified electrode for probing sialic acid through boronic acid-diol recognition. *Biosens. Bioelectron*. **2014**, *60*, 231-236.

(23) Zhou, Y.; Dong, H.; Liu, L.; Hao, Y.; Chang, Z.; Xu, M. Fabrication of electrochemical interface based on boronic acid-modified pyrroloquinoline quinine/reduced graphene oxide composites for voltammetric determination of glycated hemoglobin. *Biosens. Bioelectron*. **2015**, *64*, 442-448.

(24) Stuart, M. A. C.; Huck, W. T. S.; Genzer, J.; Müller, M.; Ober, C.; Stamm, M.; Sukhorukov, G. B.; Szleifer, I.; Tsukruk, V. V.; Urban, M.; Winnik, F.; Zauscher, S.; luzinov, I.; Minko, S. Emerging applications of stimuli-responsive polymer materials. *Nat. Mater.* **2010**, *9*, 101-113.

(25) Hu, J.; Liu, S. Responsive polymers for detection and sensing applications: current status and future developments. *Macromolecules* **2010**, *43*, 8315-8330.

(26) Zhai, L. Stimuli-responsive polymer films. *Chem. Soc. Rev.* **2013**, *42*, 7148-7160.

(27) Matsumoto, A.; Yamamoto, K.; Yoshida, R.; Kataoka, K.; Aoyagic, T.; Miyahara, Y. A totally synthetic glucose responsive

gel operating in physiological aqueous conditions. *Chem. Commun.* **2010**, *46*, 2203-2205.

(28) Ding, S.; Cao, S.; Zhu, A.; Shi, G. Wettability Switching of Electrode for Signal Amplification: Conversion of Conformational Change of Stimuli-Responsive Polymer into Enhanced Electrochemical Chiral Analysis. *Anal. Chem.* **2016**, 12219-12226**.**

(29) Zhang, X.; Shi, F.; Yu, X.; Liu, H.; Fu, Y.; Wang, Z.; Jiang, L.; Li, X. Polyelectrolyte multilayer as matrix for electrochemical deposition of gold clusters: toward super-hydrophobic surface. *J. Am. Chem. Soc.* **2004**, *126*, 3064-3065.

(30) Wang, L.; Guo, S.; Hu, X.; Dong, S. Facile electrochemical approach to fabricate hierarchical flowerlike gold microstructures: Electrodeposited superhydrophobic surface. *Electrochem. Commun.* **2008**, *10*, 95-99.

(31) Zhou, F.; Hu, H.; Yu, B.; Osborne, V. L.; Huck, W. T. S.; Liu, W. Probing the responsive behavior of polyelectrolyte brushes using electrochemical impedance spectroscopy. *Anal. Chem.* **2007**, *79*, 176-182.

(32) Motornov, M.; Sheparovych, R.; Katz, E.; Minko, S. Chemical Gating with Nanostructured Responsive Polymer Brushes: Mixed Brush *versus* Homopolymer Brush. *ACS Nano* **2008**, *2*, 41–52.

(33) Zhou, J.; Wang, G.; Hu, J.; Lu, X.; Li, J. Temperature, ionic strength and pH induced electrochemical switching of smart polymer interfaces. *Chem. Commun.* **2006**, 4820-4822.

(34) Zhu, A.; Liu, Y.; Rui, Q.; Tian, Y. Selective and sensitive determination of hydroxyl radicals generated from living cells through an electrochemical impedance method. *Chem. Commun.* **2011**, *47*, 4279-4281.

(35) Cao, H.; Yang, D.; Ye, D.; Zhang, X.; Fang, X.; Zhang, S.; Liu, B.; Kong, J. Protein-inorganic hybrid nanoflowers as ultrasensitive electrochemical cytosensing Interfaces for evaluation of cell surface sialic acid. *Biosens. Bioelectron.* **2015**, *68*, 329-335.

(36) La Belle, J. T.; Gerlach, J. Q.; Svarovsky, S.; Joshi, L. Label-free impedimetric detection of glycan-lectin interactions. *Anal. Chem.* **2007**, *79*, 6959-6964.

(37) Katz, E.; Willner, I. Probing biomolecular interactions at conductive and semiconductive surfaces by impedance spectroscopy: routes to impedimetric immunosensors, DNA-sensors, and enzyme biosensors. *Electroanalysis* **2003**, *15*, 913-947.

(38) Ding, P.; Li, X.; Qing, G.; Sun, T.; Liang, X. Disaccharide-driven transition of macroscopic properties: from molecular recognition to glycopeptide enrichment. *Chem. Commun.* **2015**, *51*, 16111-16114.

(39) Bapat, A. P.; Roy, D.; Ray, J. G.; Savin, D. A.; Sumerlin, B. S. Dynamic-covalent macromolecular stars with boronic ester linkages. *J. Am. Chem. Soc.* **2011**, *133*, 19832-19838.

(40) Malagié, I.; Trillat, A. C.; Bourin, M.; Jacquot, C.; Hen, R.; Gardier, A. M. 5-HT1B Autoreceptors limit the effects of selective serotonin re-uptake inhibitors in mouse hippocampus and frontal cortex. *J. Neurochem.* **2001**, *76*, 865-871.

(41) Paxinos, G.; Franklin, K. B. J. The mouse brain in stereotaxic coordinates, Academic Press: New York, 2001.

(42) Minami, T.; Minamiki, T.; Hashima, Y.; Yokoyama, D.; Sekine, T.; Fukuda, K.; Kumaki, D.; Tokito, S. An extended-gate type organic field effect transistor functionalised by phenylboronic acid for saccharide detection in water. *Chem. Commun.* **2014**, *50*, 15613-15615.

(43) Wang, L.; Qiao, J.; Liu, H.; Hao, J.; Qi, L.; Zhou, X.; Li, D.; Nie, Z.; Mao, L. Ratiometric fluorescent probe based on gold nanoclusters and alizarin red-boronic acid for monitoring glucose in brain microdialysate. *Anal. Chem.* **2014**, *86*, 9758-9764.

(44) Li, A.; Wang, J.; Wang, F.; Jiang, Y. Anion complexation and sensing using modified urea and thiourea-based receptors. *Chem. Soc. Rev.* **2010**, *39*, 3729-3745.

(45) Schauer, R. Sialic acids: chemistry, metabolism, and function, Springer: New York, **1982**.

(46) Mitchell, J. A.; Whitfield, J. H.; Zhang, W. H.; Henneberger, C.; Janovjak, H.; O'Mara, M. L.; Jackson, C. J. Rangefinder: A semi-synthetic FRET sensor design algorithm. *ACS Sens.* **2016**, *1*, 1286-1290.

(47) Parker, R. B.; Kohler, J. J. Regulation of intracellular signaling by extracellular glycan remodeling. *ACS Chem. Biol.* **2010**, *5*, 35-46.

(48) Marzouk, S. A. M.; Ashraf, S. S.; Al Tayyari, K. A. Prototype amperometric biosensor for sialic acid determination. *Anal. Chem.* **2007**, *79*, 1668-1674.

(49) Wang, B.; Brand-Miller, J. The role and potential of sialic acid in human nutrition. *Eur. J. Clin. Nutrition* **2003**, *57*, 1351-1369.

for TOC only